

# Practical guidelines on modelling electric engine cooling with SPH

Georg A. Mensah, Pierre Sabrowski, and Tobias B. Wybranietz,  
Dive solutions GmbH  
Berlin, Germany  
mensah@dive-solutions.de, wybranietz@dive-solutions.de

**Abstract** — Electric engines are becoming increasingly important for our transport systems and, thus, is their simulation. The smoothed-particle hydrodynamics (SPH) method is already established as a simulation tool for drivetrain technologies. This is especially true for the prediction of the lubrication flow in gearings. Hence electric engines with their moving parts also lend themselves to an SPH approach. Particularly, due to the rotor and a diverse set of cooling scenarios involving free surface flows, e.g., in jets, sprays and films. The naïve approach would be to solely introduce a proper energy equation modelling heat conduction. However, heat transfer is a complex phenomenon and, hence, such a simulation requires scrutiny. First of all, to ensure a reliable analysis, the wetting of the involved surfaces needs to be predicted correctly. This poses certain challenges to an SPH-based model: (i) the wiring of the engine coils effectively presents a rippled surface [1]. Therefore, a particle shifting procedure [2] or other means to mitigate tensile instabilities are necessary. (ii) the wetting critically depends on a good surface tension model [3, 4]. (iii) the viscosity of many coolant oils dramatically changes with temperature, in turn affecting the maximum admissible time step of the simulations. Moreover, (iv) resolving the thermal boundary layers may require local refinement techniques [5]. This paper discusses these and other challenges on the example of electric engine cooling. As this use case is of increasing interest to the from an industrial context, the presented findings may be useful for scholars and practitioners alike when formulating requirements to an SPH-solver suitable for this application.

## I. INTRODUCTION

The smoothed particle hydrodynamics (SPH) method was originally devised to model astronomical phenomena [6,7]. Since then, the method has been continuously improved and adapted as a simulation tool for other applications. Most importantly, it is utilized as a method to predict violent free surface flow and has been frequently applied in the analysis of coastal and naval hydrodynamics. For instance, to predict dam breaks, understand tsunami generation, or model wave breakers [8,9,10]. However, in recent years mechanical engineering is increasingly becoming an area of focus in the community. Especially in the domain of gear box engineering a small but thriving community of commercial SPH tools has emerged [11, 12, 13, 14]. While simulating aspects of gear box lubrication such as a proper wetting or power loss predictions with the SPH method is now state of the art, assessing the thermal management of entire assembly groups is at the cutting edge of this domain.

In general, the computational assessment of thermal management has always been an intricate task in

engineering. This is due to the various mechanisms that may contribute to a change in temperature of a device. Traditionally three mechanisms are distinguished. They are shown in Figure 1:

- Conduction  
The transfer of heat within a medium, due to molecular interactions.
- Advection  
The transfer of heat, due to a bulk motion of a fluid medium.
- Radiation  
The transfer of heat due to the emission and absorption of electromagnetic waves.

Advection cannot occur without conduction. Hence, the term convection is used to refer to heat transfer in fluid flows (not including radiation).



Figure 1: Examples of the three types of heat transfer.

Convective heat transfer may be further distinguished as *free* or *forced* depending on whether the fluid motion mainly occurs naturally because of thermal buoyancy or is generated by some sort of propeller, respectively.

Because heat transfer is such a complex topic a state-of-the-art technique is to describe the systems under consideration in terms of so-called thermal network models. In the simplest case these are sets of ordinary differential equation where the spatial dimension is addressed by lumping the system components together into network elements. Such elements may be components such as walls, gears, shafts, the engine oil, the environment, or subcomponents of these. The network approach basically formulates a model by connecting these elements via simple often linear input-output relations. These relations are linking the temperature difference from the input and output to the heat transfer rate of the elements, i.e., they are essentially descriptions of the heat transfer coefficient (HTC). For many of such components empirical relations are well known and documented in terms of non-dimensionalized formulae. A famous example is the heat transfer from fluid to a vertical

wall which can be expressed in terms of the Grashoff number and the Prandtl number, or the Reynolds number and the Prandtl number depending on whether the convection is free or forced [15]. For the conduction of heat through simple solid shapes like cylinders or blocks, the relations can even be found analytically. The thermal network approach has been successfully applied to the prediction of components in academic gearings [16] and electric vehicle engines [17]. Nevertheless, thermal networks of industrial configurations often include elements for which no relations are readily available. This is especially true for the convective elements. In order to still benefit from the low computational costs of network models accompanying computational fluid dynamics (CFD) studies need to be conducted, to characterize the HTC of convective elements. This is where SPH methods come into play.

This paper focuses on electric engine cooling with the automotive industry currently serving as the main driver for innovation in this technology. This is because unlike combustion engines, there is no broad decade-long experience with this type of engines in cars and other vehicles. A special challenge of electric engines built into vehicles is that they need to fit into a relatively small mounting space while providing a quite high power of a few hundred kW. This combination results in relatively high power densities that require some active cooling concept. One concept would be to put some coolant oil on the engines. This oil may also serve as a lubricant for the power train. The deployed oils usually feature a low contact angle to maximize the wetting of the engine components and hence both the heat transfer and the lubrication. Note that in oil-cooled electric engines a significant amount of the heat is transferred to the fluid between the coil windings. Because of the low contact angle and the narrow dimensions, applying a proper surface tension model is necessary to correctly predict how coolant oil is seeping between the windings. Additionally, local refinement may be necessary to accurately model the flow and, thus, the heat transfer in the narrow gaps between the windings. The aim of this report is to highlight best practices for the prediction of the temperature of coolant oil in an electric engine using a state-of-the-art commercial SPH simulation tool. The remainder of the paper is organized as follows. A brief section introduces the underlying model and its SPH discretization. Two validation cases are used to showcase the model: A first test case comprises a rather academic set-up where a jet of coolant oil is sprayed on a surface that is designed to mimic a compact bundle of wires in an electric engine. The second showcase is a 40kW electric engine cooled with a slow dripping flow. Remarks on the applicability of the findings and possible future developments conclude the paper.

## II. AN SPH MODEL WITH A THERMAL EQUATION

Fluid flow is commonly modelled by the Navier stokes equations. For the current work a weakly compressible

approach is used. This is a combination of a compressible equation for the conservation of mass:

$$\rho \frac{d\rho}{dt} = -\rho \nabla \cdot \vec{v},$$

and an incompressible momentum balance:

$$\rho \frac{d\vec{v}}{dt} = -\nabla p + \nabla \cdot (\mu(\nabla \otimes \vec{v} + (\nabla \otimes \vec{v})^T)) + \rho \vec{g}.$$

Here  $\rho$  is the density,  $\vec{v}$  the velocity,  $\mu$  the dynamic viscosity, and  $\vec{g}$  the gravitational acceleration. To set up the basic numerical weakly compressible SPH (WCSPH) scheme, the compact  $C^2$  Wendland kernel [18]  $w$  is used, which is defined with the smoothing length  $h$  by:

$$w_{ab} = w(\mathbf{x}_{ab}) = \begin{cases} \frac{\alpha_N}{h^N} \left(1 - \frac{q}{2}\right)^4 (1 + 2q) & , q \leq 2 \\ 0 & , q > 2 \end{cases},$$

$$\alpha_1 = \frac{3}{4}, \quad \alpha_2 = \frac{7}{4\pi}, \quad \alpha_3 = \frac{21}{16\pi},$$

where  $N$  indicates the number of dimensions and the normalized center point distance  $q$  is calculated by  $q = \|\mathbf{x}_a - \mathbf{x}_b\|/h = \|\mathbf{x}_{ab}\|/h$ . The indices  $a$  and  $b$  denote the respective properties of the considered particle and its neighboring particles. Based on the previous notations, an arbitrary scalar  $f_a$  or vector  $\mathbf{f}_a$  for particle  $a$  is approximated by the Riemann sum over the neighboring particles as [19, 20]:

$$f_a = \frac{1}{\gamma_a} \sum_b f_b V_b w_{ab}, \quad \mathbf{f}_a = \frac{1}{\gamma_a} \sum_b \mathbf{f}_b V_b w_{ab}.$$

Here  $V$  is particle volume and  $\gamma$  is the boundary renormalization factor, which involves the part of the kernel support outside the considered domain. The domain boundary shape is represented by a finite number of triangles in 3D and is included in the SPH interactions by the algorithm proposed in [21]. This type of boundary treatment is used for a WCSPH scheme in [12].

To describe the relevant surface tension phenomena, a continuum surface forces (CSF) model is added, which is oriented towards the approaches in [3] and [4]. This leads to an additional force term in the momentum balance as follows:

$$\rho \frac{d\vec{v}}{dt} = -\nabla p + \nabla \cdot (\mu(\nabla \otimes \vec{v} + (\nabla \otimes \vec{v})^T)) + \rho \vec{g} + \sigma \kappa \mathbf{n},$$

where  $\sigma$  is the surface tension coefficient,  $\kappa$  is the curvature and  $\mathbf{n}$  is the normal of the fluid surface.

When modelling fluid dynamics, particles follow their path lines, which can lead to non-uniform particle distributions and unintended clumping. This decreases the numerical quality and stability, especially near free surfaces and

complex moving geometries. To address this problem, a particle shifting scheme is applied, which is inspired by the proposed procedures in [2] and [22].

If thermal management is to be modeled, an energy equation for the prediction of the temperature is needed. In the simplest case this would be a diffusion equation based on Fourier's law of heat conduction:

$$\rho c_p \frac{dT}{dt} = \nabla \cdot (\lambda \nabla T),$$

where  $c_p$  and  $\lambda$  are the specific heat capacity and the thermal conductivity of the fluid, respectively. If necessary extra source terms may be included in this equation to model temperature changes due to viscous effects, chemical reactions, or electromagnetic heating. Note that here the Lagrangian frame of reference that is typically used when discretizing with a SPH approach naturally enforces a convection model, once such an energy equation is added to the set of model equations.

The heat equation requires the setting of appropriate thermal boundary conditions. Classic conditions are:

- Temperature boundary conditions  
Here the wall temperature is prescribed directly:  
 $T_{\text{wall}} = T.$
- Heat flux boundary conditions  
Here the heat flux is prescribed at the walls using Fourier's law:  $q_{\text{wall}} = \lambda \nabla T \cdot \vec{n}.$
- Convective boundary condition  
This condition prescribes a local HTC:  
 $h(T_{\text{wall}} - T_{\text{ref}}) + \lambda \nabla T_{\text{wall}} \cdot \vec{n} = 0.$

Note that these 3 conditions are of Dirichlet, Neumann, and Robin type respectively. They lend themselves to an implementation via a single generic interface that is parametrized as  $a T_{\text{wall}} + b \nabla T_{\text{wall}} \cdot \vec{n} = c.$

It is common practice to model the lighter phase in an SPH simulation by not discretizing it with particles at all. For instance, in electric engine cooling applications this means that the coolant oil is discretized as particles while the air is represented as an empty void. This approach results in drastically faster simulation times, but obviously introduces an extra modelling error. For the modelling of heat the approach implies that the ignored phase acts as a perfect insulator. This is because the void that represents the neglected phase can neither store nor transfer any heat. However, this does not mean that the void cannot be assigned a temperature. Indeed, an air temperature is necessary to obtain estimates of the temperature at a point where an interpolation kernel is not fully filled, i.e. the particle density as expressed by the local Shepard summation  $s_a = 1/\gamma_a \sum_b V_b w_{ab}$  is less than  $s_a < 1.$  However, the simplification here is that the air temperature

is constant. In particular, such neglected-phase models require special care when interpreting assigned heat flux boundary conditions. For example, if there is a wall that is not wetted at all, it cannot transfer any heat even if a heat flux boundary condition is prescribed there. In general, such a neglected-phase model implies an effective boundary condition:  $s_a q_{\text{wall}} = \lambda \nabla T \cdot \vec{n}.$  Therefore, it is important to predict the wetting accurately. This entails that when running a neglected-phase model special care is necessary to predict the wetting correctly, in order to not further compromise on the transferred heat. Note, that a viable workflow is to first calculate the level of wetting in terms of the Shepard summation and then scale the heat flux accordingly in a subsequent simulation.

Another major challenge in the validation cases studied here is to capture the thermal boundary layer to accurately predict the heat transfer. For this purpose, an adaptive particle refinement (APR) technique [5] is utilized to resolve the thin boundary layers along the profile of the component geometries, as shown in Figure 2.

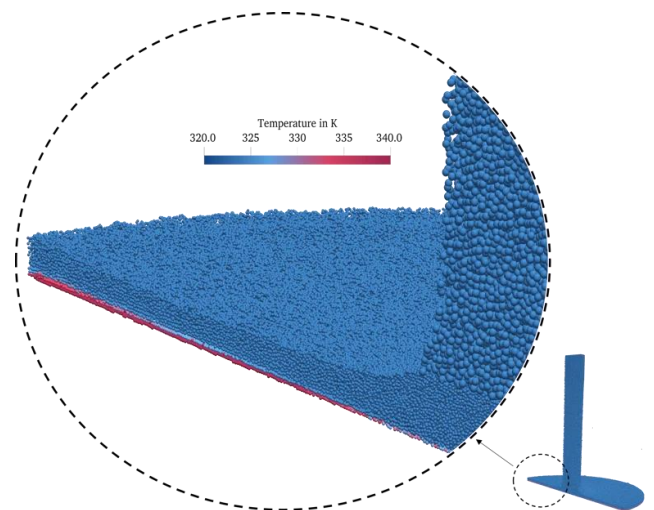


**Figure 1.2** Use of the APR technique in the near-wall region to resolve the thermal boundary layer.

### III. VALIDATING THE THERMAL SPH MODEL

To test the quality of the implementation a case taken from [23] has been simulated. The set-up is rather simple. A nozzle sprays oil onto a target. In the original study in addition to a flat surface various surface geometries that are representative of electric engine wire bundles have been studied. This has been achieved by carving a series of parallel ridges with featuring a rounded cross section into the surface of the target. As this design aims to mimic the surface of a compact wire bundle, the diameters of the ridges have been chosen to correspond to radii from the American wire gauge (AWG). As a coolant oil automatic transmission fluid (ATF) has been used, namely Ford's Mercon LV ATF. This choice renders the study a good validation case for automotive applications. The original work is purely

experimental and reports the measured HTC. Validation then consists of simulating various represented operating points and comparing the results to the reported values.

The simulations in this report model the test with a flat surface and a carved surface mimicking 26AWG wire bundle, i.e., the ridges feature a radius of 0.404mm. The configuration is shown in Figure 3.1.

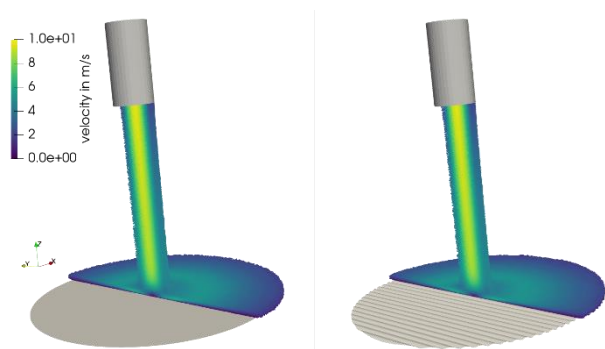


**Figure 3.1** Geometry used in the test simulation. Coolant Oil at 50°C is sprayed on a 110°C surface. Two cases have been studied. A perfectly flat surface (left) and a rippled surface modelled to represent a compact 26 AWG wire bundle.

The inlet temperature is 50°C while the surface temperature is 110°C. More details concerning the geometry can be found in the original work [23]. Mean inlet velocities of 0.5 m/s, 5 m/s, and 10 m/s have been simulated and compared to the experimental results. Particle diameters of 0.1 mm and 0.05 mm were tested. For both cases simulations with and without an extra particle refinement zone that additionally reduces the diameter of particles close to the target by an extra factor of two were conducted. In total this results in an array of 24 test simulations. The temperature field for the finest resolution and a mean inlet velocity of 5 m/s is shown in Figure 3.2.



**Figure 3.2** Results of the flow simulation for a 26AWG surface for a mean inlet velocity of 5 m/s and local refinement close to the target surface (0.050 mm diameter for the coarse particles and 0.025 mm for the fine particle). In comparison to Figure 3.1 this shows a view from the bottom in order to visualize the fluid temperature at the flat (left) and 26 AWG (right) surface.

Comparison of the HTCs obtained in these simulations with the experimental results is shown in Figure 3.3.

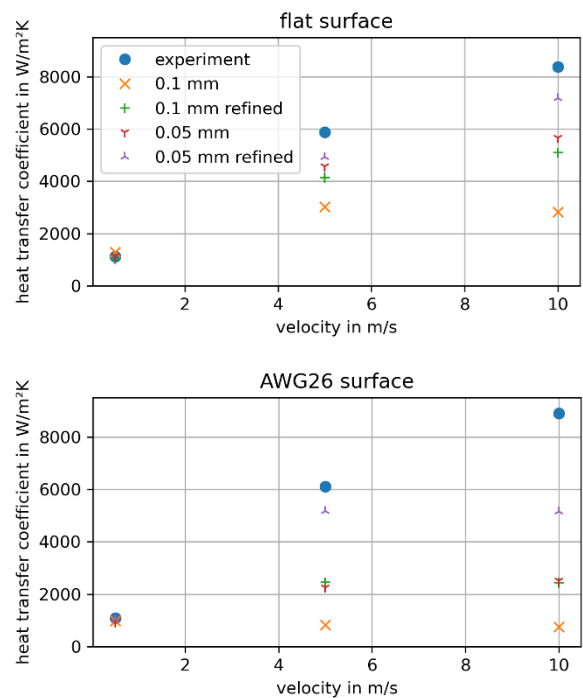


**Figure 3.3** Comparison of HTCs obtained from simulations with a flat surface (top) and an 26AWG surface (bottom) for various inlet velocities. The simulations comprise different particle resolutions and may use an extra level of local refinement close to the target surface.

For an inlet velocity of 0.5 m/s the HTC can be computed accurately for both the flat and the AWG26 surface with all particle resolutions. However, when increasing the inlet velocity the results start deviating from the experimental ones. In the case of the flat surface, the HTCs computed with a particle diameter of 0.1 mm are almost the same for inlet velocities of 5m/s and 10m/s. That the computational results are independent of the inlet velocity suggests that the simulation is under resolved. Indeed, the estimated coefficients become more accurate if the resolution is increased, with the best predictions being obtained when having 0.05 mm and additional local refinement. In the case of the flat surface the simulations then predict the trend of the HTCs correctly and even for an inlet velocity of 10m/s the computation only deviates from the experiment by about 15%. For the 26AWG surface, however, only the results for 0.5m/s and 5m/s can be considered satisfactory. When having an inlet velocity of 10m/s the computed results do not differ much from the prediction obtained for 5m/s. This indicates that the resolution of the particles is not sufficient to resolve the flow behavior between the ridges at such high speeds.

This test case underlines the importance of correctly resolving the geometrical features and adjacent boundary layers by choosing an appropriate (local) particle size. Unsurprisingly, this challenge is getting more and more difficult at increasing velocities. The issue is of course not exclusive to SPH models but inherent to the modeling of

fluid flows. In addition to local refinement techniques traditional grid-based CFD has, therefore, developed wall-function techniques. This is assuming a shape for the viscous and thermal boundary layers and deriving from that assumption a more accurate numerical boundary condition that compensates for a too coarse resolution. Although not done here, the concept may also be used to improve the quality of SPH models.

#### IV. E-ENGINE TEST CASE

As a more complex validation case data from an experimental study of an oil-cooled electric engine has been used [24]. The engine is a 40kW radial flux machine featuring 12 coils. Details on the geometry can be found in the original reference. While this paper focuses on a set-up that uses 5 inlets to drip oil on the coil windings, it is worth noting that the original experimental study also encompassed other injection concepts like flat or cone spray nozzles to generate jets or mist, respectively. Although not done in the present study, these other configurations may serve as interesting test cases in future works. Because the experimental set-up is symmetric, the simulation comprises only half of the domain and appropriate boundary conditions are imposed on the symmetry plane. These are slip-flow, zero heat flux and  $90^\circ$  contact angle. The set-up is illustrated in Figure 4.1.

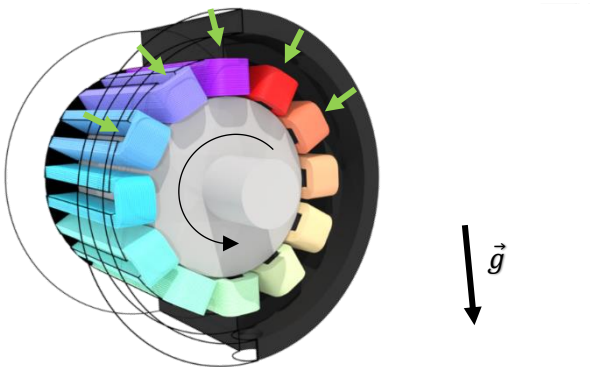


**Figure 4.1** Computational set-up. Five orifices distribute coolant oil on the five coils on the top. The position of the orifices is highlighted by the green arrows. The twelve coils are highlighted in various colors and do not move. The rotor (light gray) rotates with a constant rotational speed of 2750 rpm. The image only shows one half of the entire engine. Appropriate symmetry boundary conditions are therefore applied on the back of the set-up.

For a rotational speed of 2750 rpm three different inlet mass flows have been simulated, viz. 110 l/h, 220 l/h and 368 l/h. The exact properties of the coolant oil are not given in the original work, which is why typical values were assumed. These are a density of  $930.0 \text{ kg/m}^3$ , a thermal conductivity of  $0.145 \text{ K/m}$ , and a specific heat capacity of  $2000 \text{ J/(kgK)}$ . A surface tension coefficient of  $0.03 \text{ m/N}$  and a contact angle of  $30^\circ$  at all surfaces were also assumed. The viscosities at  $50^\circ\text{C}$  ( $30\text{E-}6 \text{ m}^2/\text{s}$ ) and  $75^\circ\text{C}$  ( $12\text{E-}6 \text{ m}^2/\text{s}$ ) were reported in the original work. Viscosities at other temperatures were computed using the following exponential law

$$v(T) = v_{50^\circ\text{C}} \times \exp\left(\log\left(\frac{v_{75^\circ\text{C}}}{v_{50^\circ\text{C}}}\right) \times \frac{T - 50}{75 - 50}\right),$$

where the temperature must be given using the Celsius scale. Except for the coils all surfaces were assumed to be adiabatic. For the coils a temperature boundary condition of  $110^\circ\text{C}$  was set. The inlet temperature of the oil was  $75^\circ\text{C}$ . The simulation was initialized without any oil in the computational process, i.e., the simulation also covers a filling phase in which oil accumulates between the coils and in an oil sump at the bottom of the engine. The simulation covered the first 7.5s of the cooling process and was carried out with a particle diameter of 0.6mm. The figures 4.2 to 4.7 show the velocity and temperature fields of the coolant oil at  $t=7.5\text{s}$  for the three tested flow rates.

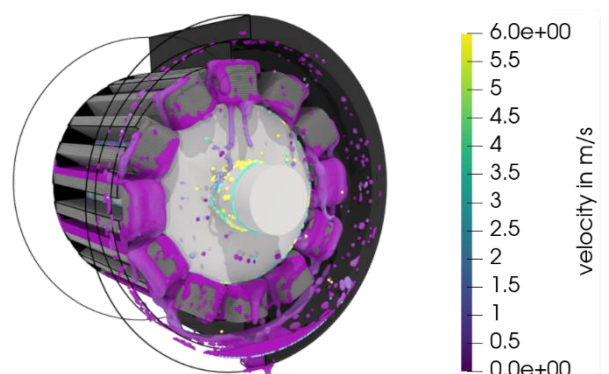


**Figure 4.2** Velocity of the coolant oil in the engine at 7.5s for a flow rate of 110 l/h.

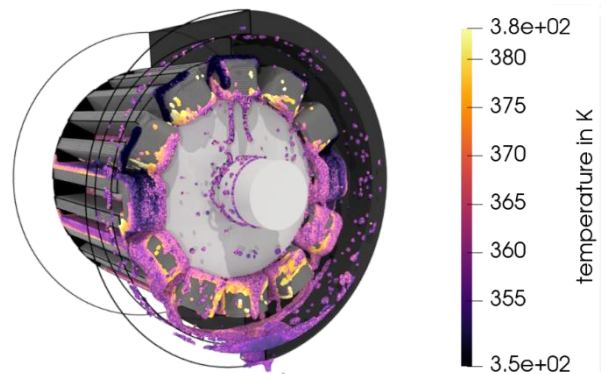


**Figure 4.3** Temperature of the coolant oil in the engine at 7.5s for a flow rate of 110 l/h.

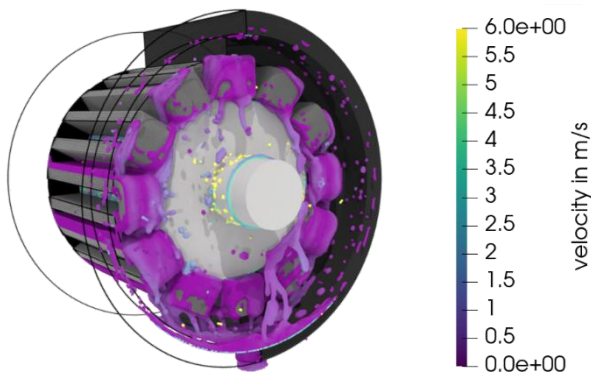


Figure 4.4 Velocity of the coolant oil in the engine at 7.5s for a flow rate of 220 l/h.

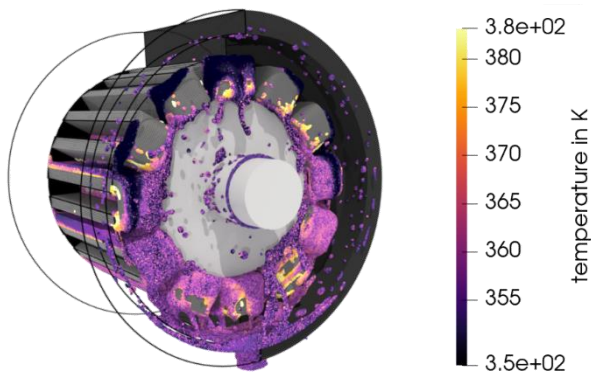


Figure 4.5 Temperature of the coolant oil in the engine at 7.5s for a flow rate of 220 l/h.

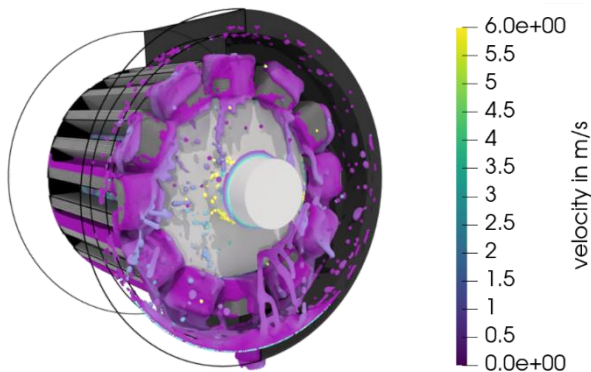


Figure 4.6 Velocity of the coolant oil in the engine at 7.5s for a flow rate of 368 l/h.

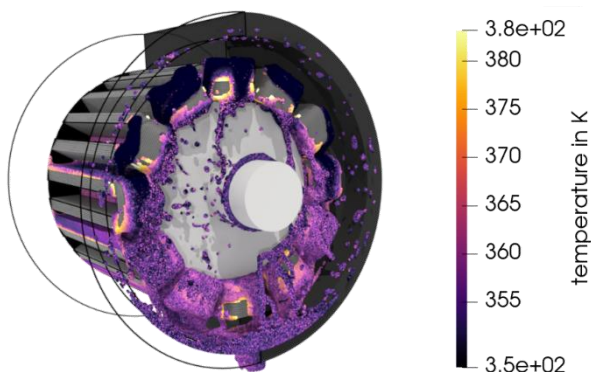


Figure 4.7 Temperature of the coolant oil in the engine at 7.5s for a flow rate of 368 l/h.

The evolution of the heat transfer rate of the 12 coil surfaces over time for the three mass flow rates is depicted in Figure 4.8. The results indicate that for a mass flow rate of 110 l/h the time span of 7.5 s is not sufficient to reach a steady state. However, for the flow rates of 220 l/h and 368 l/h the heat transfer rate does not change anymore after about 4s. The heat transfer rates found at 7.5 s for the three flow rates are 800 W, 1100 W, and 1350 W, respectively. As compared to the rates reported in the experiment (560W, 650W, and 730W) they deviate by a factor of 1.42 to 1.85. Given the assumptions of the model, i.e., the negligence of heat transfer in the solid and gas phase, the assumption for the properties of the fluid, and the simplistic boundary conditions, these are considered to be satisfactory.

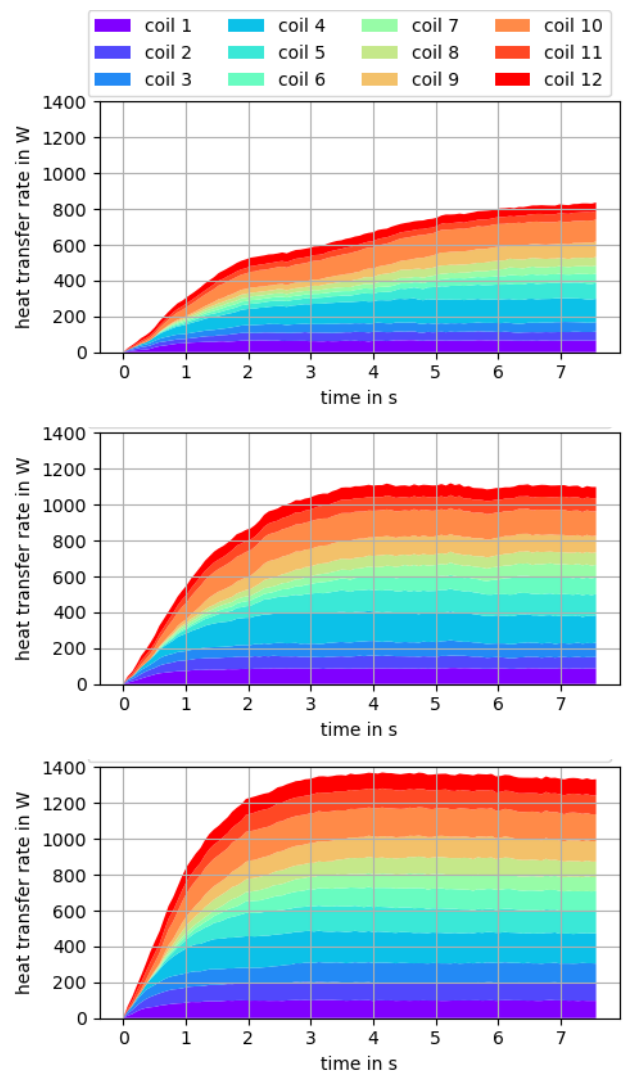


Figure 4.8 Cumulated plot of the transfer rate from the coils to the coolant oil for a flow rate of 110 l/h (top), 220 l/h (middle), and 368 l/h. The colors indicate the share the individual coils have on the total heat transfer. They correspond to the colors in Figure 4.1.

## V. CONCLUSIONS AND OUTLOOK

The challenges of using an SPH approach for the prediction of the cooling effect in oil-cooled electric engines were discussed. A generic test case underlines the importance of a good boundary model. This regards both, its geometric representation in the simulation and the correct resolution of adjacent boundary layer. A practical example of an electric engine demonstrates that reasonable results for the heat transfer can be obtained from an SPH model. Future work will focus on the development of more efficient models for the boundary layer modelling using more advanced local refinement approaches [25] and the implementation of wall functions. Moreover, a better representation of the air phase will be considered.

### ACKNOWLEDGEMENTS

We thank Sascha Thiede, Shriram Krishna, and Leonid Braun for their support in this work.

### References

- [1] Bennion, K. and Moreno, G., "Convective Heat Transfer Coefficients of Automatic Transmission Fluid Jets with Implications for Electric Machine Thermal Management," preprint, <https://www.nrel.gov/docs/fy15osti/63969.pdf>, 2015
- [2] Lyu, H. G., & Sun, P. N. "Further enhancement of the particle shifting technique: Towards better volume conservation and particle distribution in SPH simulations of violent free-surface flows" *Applied Mathematical Modelling*, 101, pp. 214-238, 2022
- [3] Vergnaud, A. "Améliorations de la précision et de la modélisation de la tension de surface au sein de la méthode SPH, et simulations de cas d'amerrissage d'urgence d'hélicoptères", Doctoral dissertation, École centrale de Nantes, 2022.
- [4] Bierwisch, C., "Consistent Thermo-Capillarity and Thermal Boundary Conditions for Single-Phase Smoothed Particle Hydrodynamics. *Materials*", 14:4530, 2021.
- [5] Chiron, L., Oger, G., De Leffe, M., & Le Touzé, D., "Analysis and improvements of Adaptive Particle Refinement (APR) through CPU time, accuracy and robustness considerations" *Journal of Computational Physics*, 354, pp. 552-575, 2018
- [6] Gingold, R. A. and Monaghan, J. J., "Smoothed particle hydrodynamics: theory and application to non-spherical stars. *Monthly notices of the royal astronomical society*", 181(3), pp. 375-389, 1977.
- [7] Lucy, L. B., "A numerical approach to the testing of the fission hypothesis. *The astronomical journal*", 82, pp. 1013-102, 1977
- [8] Monaghan, J. J. "Simulating free surface flows with SPH. *Journal of Computational Physics*", 110(2), pp. 399-406, 1994.
- [9] Dalrymple, R. A. and Rogers, B. D. "Numerical modeling of water waves with the SPH method. *Coastal Engineering*", 53, pp. 141-147, 2006.
- [10] Barreiro A. et al, "Smoothed Particle Hydrodynamics for coastal engineering problems", *Computers and Structures* 120, pp. 96-106, 2013.
- [11] Z. Ji, M. Stanic, E. A. Hartono and V. Chermoray, "Numerical simulations of oil flow inside a gearbox by Smoothed Particle Hydrodynamics (SPH) method," *Tribology International*, vol. 127, pp. 47-58, 2018.
- [12] P. Sabrowski, L. Beck and T. B. Wybraniec, "Modern WCSPH in industrial multiphase application considering complex moving boundaries", *Proceedings of the 14th International SPHERIC Workshop*, pp. 266-273, 2018.
- [13] M. C. Keller, S. Braun, L. Wieth, G. Chaussonnet, T. F. Dauch, R. Koch, C. Schwitzke and H. J. Bauer, "Smoothed particle hydrodynamics simulation of oil-jet gear interaction," *Journal of Tribology*, vol. 141(7), 2019.
- [14] G. Maier, W. Baier, A. Diemath, F. Testa, "Anforderungen und Grenzen traditioneller FVM und neuer SPH-Ansätze zur Strömungssimulation in Fahrzeuggetrieben," *NAFEMS DACH Magazin*, vol. 52, pp. 42-53, 2019.
- [15] VDI Heat Atlas, Springer, 2<sup>nd</sup> international edition, ISBN: 978-3-540-77877-6, 2010
- [16] Paschold, C. et al., "Calculating component temperatures in gearboxes for transient operation conditions", *Forsch Ingenieurwes* (2022) 86, pp. 521-534, 2021
- [17] Liu, Y. et al., "Bulk temperature prediction of a two-speed automatic transmission for electric vehicles using thermal method and experimental validation", *Proc Inst Mech Eng Part D J Automob Eng* 101(3), pp. 2585-2598, 2018
- [18] Wendland, H., "Piecewise polynomial, positive definite and compactly supported radial functions of minimal degree", *Advances in Computational Mathematics*, 4, pp. 389-396, 1995
- [19] Violeau, D., "Fluid Mechanics and the SPH Method: Theory and Applications", Oxford University Press, pp. 321-327, 2012.
- [20] Feldman, J. and Bonet, J., "Dynamic refinement and boundary contact forces in SPH with applications in fluid flow problems" *International Journal for Numerical Methods in Engineering*, 72, pp. 295-324, 2007
- [21] Chiron, L. and de Leffe, M. and Oger, G. and Le Touzé, D., "Fast and accurate SPH modelling of 3D complex wall boundaries in viscous and non viscous flows", *Computer Physics Communications*, 234, pp. 93-111, 2019
- [22] Michel, J. and Vergnaud, A. and Oger, G. and Le Touzé, D. "Considerations on Particle Shifting Technique for SPH schemes", *Proceedings of the 15th International SPHERIC Workshop*, pp. 30-37, 2021.
- [23] K. Bennion and G. Moreno, "Convective heat transfer coefficients of automatic transmission fluid jets with implications for electric machine thermal management", *Int. technical conference and exhibition on packaging and integration of electronic and photonic microsystems*, 2015
- [24] T. Davin, S. Harmand, J. Pelle, "Experimental study of oil cooling systems for electric motors", *Applied Thermal Engineering* 75 (2015), 2015
- [25] Winchenbach, R. and Kolb, A., "Optimized Refinement for Spatially Adaptive SPH", *ACM Trans. Graph.* 40, Article 8, 15 pages, 2021.